Thermodynamic Properties and Phase Equilibria for Pt-Rh Alloys

K.T. JACOB, SHASHANK PRIYA, and YOSHIO WASEDA

The activity of rhodium in solid Pt-Rh alloys is measured in the temperature range from 900 to 1300 K using the solid-state cell

$$\text{Pt-Rh, Rh} + \text{Rh}_2\text{O}_3/(\text{Y}_2\text{O}_3)\text{ZrO}_2/\text{Pt}_{1-x}\text{Rh}_x + \text{Rh}_2\text{O}_3\text{, Pt-Rh}$$

The activity of platinum and the free energy, enthalpy, and entropy of mixing are derived. Activities exhibit moderate negative deviation from Raoult's law. The mixing properties can be represented by a pseudosubregular solution model in which excess entropy has the same type of functional dependence on composition as the enthalpy of mixing,

$$\Delta H = X_{\text{Rh}}\,(1 - X_{\text{Rh}})[-10{,}970 + 45X_{\text{Rh}}] \quad \text{J/mol}$$

$$\Delta S^E = X_{\text{Rh}}\,(1 - X_{\text{Rh}})[-3.80 + 1.55 \times 10^{-2}\,X_{\text{Rh}}] \quad \text{J/mol·K}$$

The negative enthalpy of mixing obtained in this study is in qualitative agreement with predictions of semiempirical models of Miedema and co-workers and Colinet *et al.* The results of this study do not support the solid-state miscibility gap suggested in the literature, but are consistent with liquidus data within experimental uncertainty limits.

I. INTRODUCTION

Alloys of platinum and rhodium are extensively used in thermocouples for high-temperature measurement and as clean and inert heating elements in experimental high-temperature furnaces. The phase diagram for the Pt-Rh system is inadequately characterized.[1] The liquidus has been measured by Müller[2] and Acken.[3] The results have been normalized using more recent values for the melting points of the two pure components.[1,4] The liquid-solid two-phase region in this isomorphous system is displaced upward with respect to the straight line joining the melting points of the pure metals Pt and Rh,[1,5] implying that the solid solution is relatively more stable than the liquid alloy. Since Pt and Rh belong to the same group of the periodic table, the behavior of the liquid phase is expected to be close to ideal. The nature of the two-phase lens would then imply negative deviation from ideality for the solid solution. However, Raub[6] has suggested the onset of solid-state immiscibility below ~1033 K, based on information for other binary systems involving platinum-group metals such as Pt-Ir, Pd-Ir, and Pd-Rh. Magnetic susceptibility data of Darling,[7] which show a sharp inflection in the susceptibility as a function of composition at $X_{\text{Rh}} \cong 0.23$, have been cited in support of this hypothesis.[8] The miscibility gap has been retained in recent phase diagram compilations,[1,5] although Raub and Falkenburgh[9] were unable to confirm the existence of a miscibility gap even after annealing for 150 days at 873 and 1073 K. The presence of a miscibility gap would require positive deviation from ideality. Thus, there is an apparent inconsistency between the measured liquidus and the inferred miscibility gap. Since studies on phase separation at low temperatures are time consuming and sometimes inconclusive because of kinetic factors, thermodynamic activities in the solid solutions are measured at temperatures above the suggested miscibility gap. Thermodynamic data can provide decisive evidence for or against solid-state immiscibility.

An important limiting factor in the use of Pt-Rh alloys is the temperature below which Rh_2O_3 can form as the stable phase. In air, pure Rh_2O_3 is stable below 1315 K.[10] The oxygen potential in equilibrium with Pt-Rh alloys and Rh_2O_3 can be readily measured using a cell incorporating stabilized zirconia as the solid electrolyte. When a mixture of Rh + Rh_2O_3 is used as the reference electrode, the electromotive force (emf) of the cell is directly related to the activity of rhodium in the alloy. The method is similar to that used by Rapp and Maak.[11] Thus, information on the activity of rhodium and the oxygen potential for the formation of Rh_2O_3 can both be obtained from the same measurement.

II. EXPERIMENTAL

A. *Materials*

Pt-Rh alloys were made by melting an Rh and Pt sponge of 99.9 pct purity on a water-cooled copper hearth under argon gas. Each alloy button was remelted four times to ensure homogeneity. Fine powders of Rh and Rh_2O_3, each of purity greater than 99.99 pct, were used to prepare the reference electrode. Alloy powders were prepared by filing. Iron particles in the powder were removed by a strong magnet. Residual iron was removed by chemical dissolution in

K.T. JACOB, Professor, and SHASHANK PRIYA, Graduate Student, are with the Department of Metallurgy, Indian Institute of Science, Bangalore 560 012, India. YOSHIO WASEDA, Professor and Head, Research Center for Metallurgical Process Engineering, is with the Institute for Advanced Materials Processing, Tohoku University, Sendai 980-8577, Japan.

Manuscript submitted August 15, 1997.

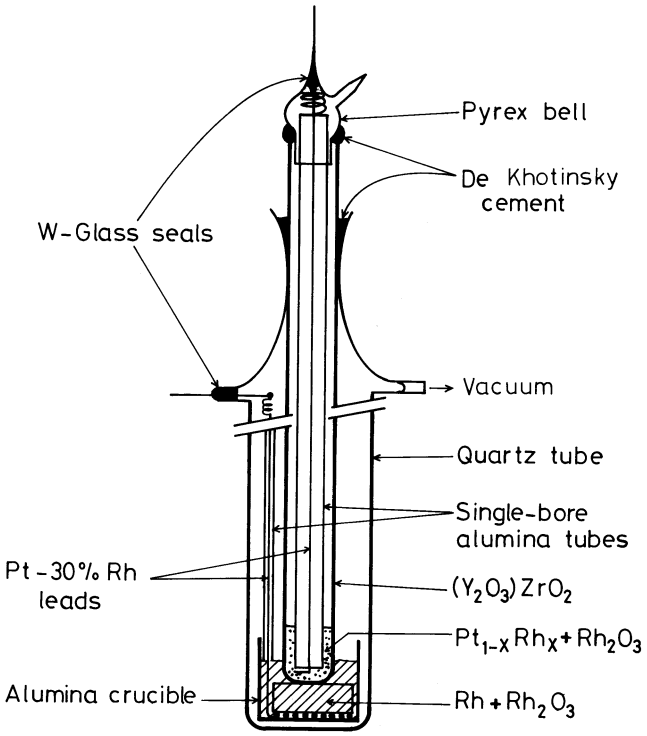

Fig. 1—Schematic diagram of the apparatus used for emf measurement.

acid. Yttria-stabilized zirconia solid electrolyte tubes were obtained from Corning Inc. (Corning, NY.).

B. *Apparatus*

A schematic diagram of the apparatus used for emf measurements on the cell,

$$\text{Pt-30 pct Rh, Rh} + \text{Rh}_2\text{O}_3 \;\big|\; (\text{Y}_2\text{O}_3)\text{ZrO}_2 \;\big|\; \text{Pt}_{1-X}\text{Rh}_X + \text{Rh}_2\text{O}_3\text{, Pt-30 pct Rh} \quad [1]$$

is shown in Figure 1. The cell is written such that the right-hand electrode is positive. The reference electrode was prepared by compacting an intimate mixture of fine powders of Rh and Rh_2O_3 in the molar ratio 1:1.5 in a steel die at 250 MPa. The pellet was sintered in an evacuated quartz ampule at 1273 K for 10 hours. The pellet was contained in an alumina crucible placed inside the ampule to avoid contamination. The reference electrode was placed on a wire grid of Pt-30 pct Rh alloy in an alumina crucible which was placed inside a larger vertical quartz tube, as shown in the diagram. A $(Y_2O_3)ZrO_2$ solid electrolyte tube with a flat, closed end was pressed against the reference electrode pellet. The annular space between the alumina crucible and the zirconia tube was filled with loose powder of Rh + Rh_2O_3, which was compacted by raming with a steel rod. The quartz tube was necked at the top end and provided with two side arms, one for evacuation and the other for an electrical lead to the reference electrode. A tungsten electrode sealed into glass was used to connect the Pt-30 pct Rh wire to a high-impedance (10^{12} Ω) digital voltmeter. An alumina sheath was used to insulate the Pt-30 pct Rh lead. The narrow gap between the zirconia tube and the neck of the quartz tube at the cold end was closed with De Khotinsky cement. The outer silica tube was then evacuated and flame sealed under vacuum.

The measuring electrode, consisting of an intimate mixture of Pt-Rh alloy and Rh_2O_3 in the molar ratio 1:1.5, was placed inside the zirconia tube with a Pt-30 pct Rh wire partially embedded in the mixture. The mixture was compacted by raming with a steel rod. A single-bore alumina tube was used to insulate the electric lead and to apply pressure on the measuring electrode. The top end of the zirconia tube was closed with a tight-fitting, bell-shaped PYREX* cap, which supported a tungsten electrode connection sealed into glass. The joint between the bell and the zirconia tube was also sealed with De Khotinsky cement. A spring placed between the bell and the alumina tube applied pressure on the measuring electrode, thus ensuring good contact between the electrodes and the solid electrolyte. The zirconia tube was evacuated through a side tube attached to the PYREX bell and flame sealed under vacuum. During measurement at high temperatures, equilibrium oxygen pressures were established inside the evacuated quartz and zirconia tubes by dissociation of Rh_2O_3 at the electrodes.

*PYREX is a trademark of Corning Inc., Corning, NY.

C. *Procedure*

The cell was placed in a vertical resistance furnace with the electrodes situated in the even-temperature zone (± 1 K). The temperature of the furnace was controlled to ± 1 K. The temperature was measured by a Pt/Pt-13 pct Rh thermocouple calibrated against the melting point of gold. The upper part of the assembly, where cement seals were located, was maintained at room temperature. A Faraday cage, made of stainless steel foil, was placed between the furnace and the cell assembly. The foil was earthed to minimize any induced emf on cell leads. The emf of the cell was measured by a digital voltmeter with a sensitivity of ± 0.01 mV. The cell was first heated to 1200 K and maintained at temperature for 10 hours to allow the alloy electrode to sinter *in situ*. Subsequently, the emf was measured as a function of temperature. To check for the presence of any thermal gradient across the cell and other stray contributions to emf, the open-circuit potential of a symmetric cell,

$$\text{Pt-30 pct Rh, Rh} + \text{Rh}_2\text{O}_3 \;\big|\; (\text{Y}_2\text{O}_3)\text{ZrO}_2 \;\big|\; \text{Rh} + \text{Rh}_2\text{O}_3\text{, Pt-30 pct Rh} \quad [2]$$

was measured as a function of temperature. The emf was found to lie in a narrow range, ± 0.05 mV, without any systematic trends.

The reversibility of cell emf was established by microcoulometic titration in both directions. A small current (~50 μA) was passed through the cell, using an external potential source, for ~5 minutes. The open-circuit emf was subsequently monitored as a function of time. The emf was found to return to the same steady value before each titration. During titration, the chemical potential of oxygen at each electrode was displaced from equilibrium by a small amount. Since the electrode potentials returned to the same value after displacement from equilibrium in opposite di-

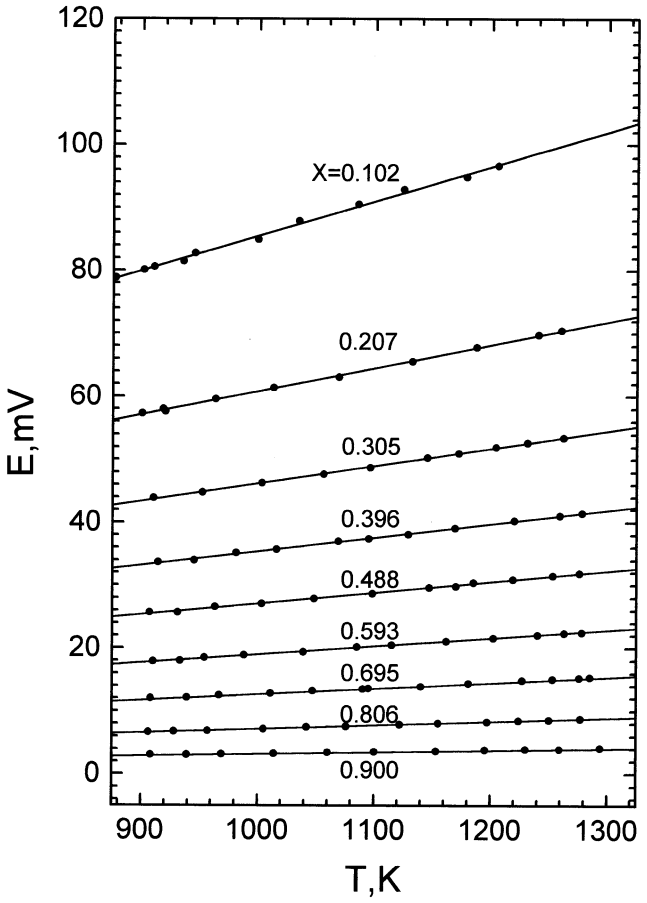

Fig. 2—Temperature dependence of the emf of the solid-state cell [1] for different alloy compositions.

rections, reversibility was confirmed. The emf was found to be reproducible on cycling the temperature of the cell. The time required to reach a steady emf varied from 2 hours at 900 K to 0.5 hours at 1250 K.

After each experiment, the electrodes were examined by X-ray diffraction (XRD) analysis. No change in the phase compositions of the electrodes was detected. There was no evidence of formation of ternary condensed phases in the Pt-Rh-O system.

III. RESULTS AND DISCUSSION

A. *Thermodynamic Properties of Solid Pt-Rh Alloys*

The reversible emf of cell [1] is plotted as a function of temperature in Figure 2 for different alloy compositions. For alloys with $X_{Rh} = 0.102$ and 0.207, the oxygen partial pressure over the alloy electrode exceeds atmospheric pressure above 1206 and 1261 K, respectively. Hence, the temperature range available for measurement was slightly reduced for these compositions. The emf increases linearly with temperature for each composition. Equations for emf, obtained by least-squares regression analysis, are summarized in Table I. The uncertainty limits correspond to twice the standard deviation. The temperature-dependent term is related to the partial molar entropy and the temperature-independent term to the partial molar enthalpy of Rh in the alloy. The activity of Rh (a_{Rh}) is related to the emf as follows:

Table I. Equations for Emf Obtained by Least-Squares Regression Analysis

X_{Rh}	E (mV)
0.102	$30.5 + 5.50 \times 10^{-2}\ T\ (\pm 0.8)$
0.207	$23.8 + 3.70 \times 10^{-2}\ T\ (\pm 0.5)$
0.305	$18.4 + 2.78 \times 10^{-2}\ T\ (\pm 0.3)$
0.396	$13.6 + 2.18 \times 10^{-2}\ T\ (\pm 0.3)$
0.488	$9.9 + 1.72 \times 10^{-2}\ T\ (\pm 0.2)$
0.593	$6.2 + 1.28 \times 10^{-2}\ T\ (\pm 0.2)$
0.695	$3.5 + 9.23 \times 10^{-3}\ T\ (\pm 0.2)$
0.806	$1.5 + 5.70 \times 10^{-3}\ T\ (\pm 0.1)$
0.900	$0.4 + 2.90 \times 10^{-3}\ T\ (\pm 0.1)$

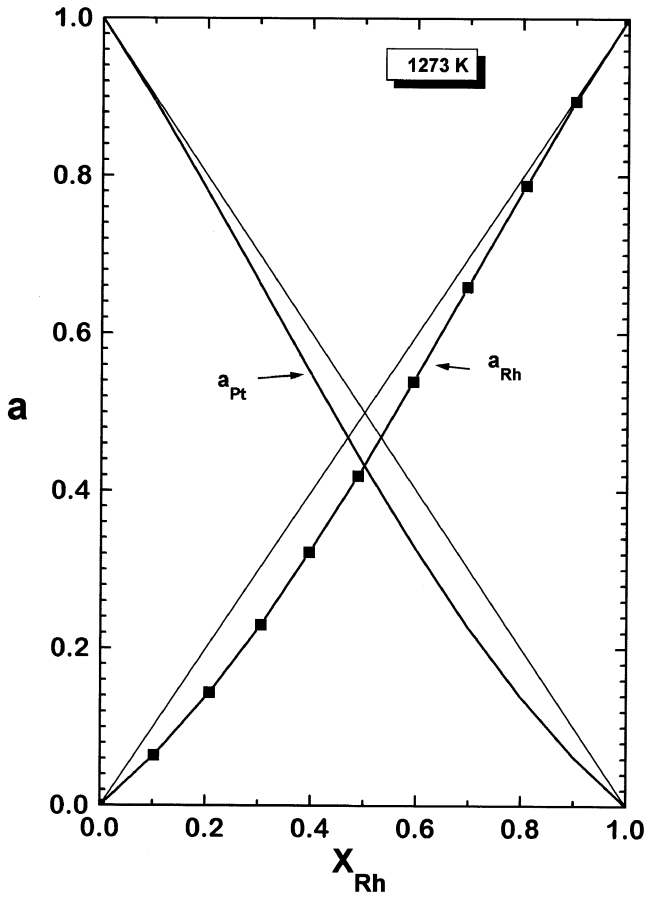

Fig. 3—Activity-composition relationships for the system Pt-Rh at 1273 K.

$$-3FE = \Delta\mu_{Rh} = \Delta G_{Rh} = RT \ln a_{Rh} \qquad [3]$$

where F is the Faraday constant, E is the emf, $\Delta\mu_{Rh}$ is the chemical potential of Rh relative to pure solid Rh, and ΔG_{Rh} is the relative partial molar free energy of Rh in the alloy. Strictly, the measured activity of Rh is for a ternary Pt-Rh-O alloy saturated in oxygen. However, since the oxygen solubility in the solid alloy is negligible (<0.01 at. pct), the effect of oxygen can be neglected. The measured activity of Rh is, therefore, representative of the binary Pt-Rh. The activity of Rh at 1273 K is plotted as a function of composition in Figure 3. The activity shows moderate negative deviation from Raoult's law. The α_{Rh} function, defined as

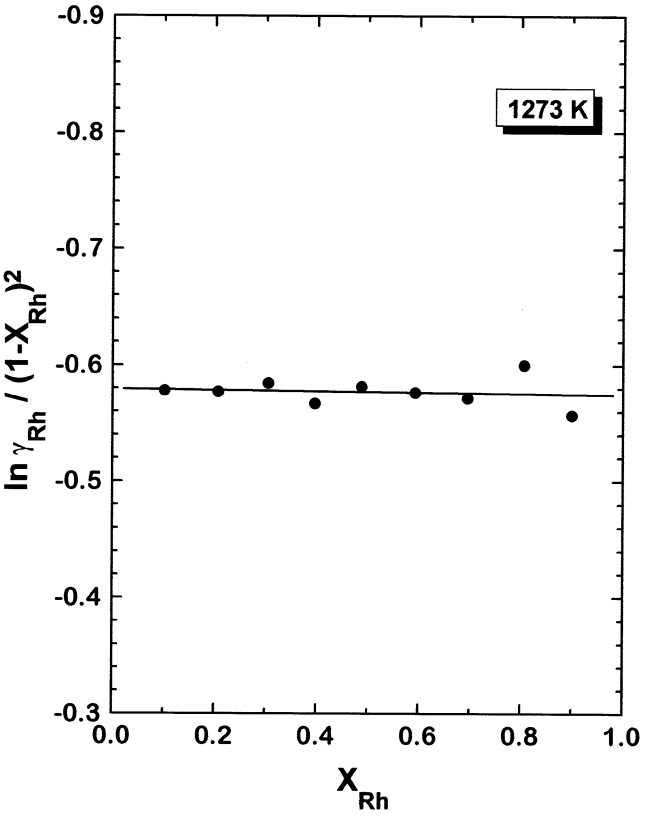

Fig. 4—Variation of the α_{Rh} function with composition for Pt-Rh alloys at 1273 K.

$$\alpha_{Rh} = \frac{\ln (a_{Rh}/X_{Rh})}{(1 - X_{Rh})^2} = \frac{\ln \gamma_{Rh}}{(1 - X_{Rh})^2} \quad [4]$$

is plotted as a function of composition in Figure 4. The values of α_{Rh} for Rh-rich alloys are associated with larger uncertainty, because the denominator of Eq. [4] rapidly decreases with an increasing value of X_{Rh}. Although an average value of α_{Rh}, independent of composition, can be used to describe the system, a better correlation is obtained if α_{Rh} is represented by a linear equation,

$$\alpha_{Rh} = -0.579 + 0.005\, X_{Rh} \quad [5]$$

The excess chemical potential or excess partial molar free energy of Rh at 1273 K is obtained from the expression for α_{Rh},

$$\Delta\mu^E_{Rh} = \Delta G^E_{Rh} = RT \ln \gamma_{Rh} = (1 - X_{Rh})^2[-6130 + 50X_{Rh}] \text{ J/mol} \quad [6]$$

From the Gibbs–Duhem equation, the excess chemical potential of Pt and the integral excess free energy of mixing of solid Pt-Rh alloys are obtained,

$$\Delta\mu^E_{Pt} = \Delta G^E_{Pt} = RT \ln \gamma_{Pt} = X^2_{Rh}\,[-6155 + 50X_{Rh}] \text{ J/mol} \quad [7]$$

$$\Delta G^E = X_{Rh}\,(1 - X_{Rh})\,[-6130 + 25X_{Rh}] \text{ J/mol} \quad [8]$$

For each composition, the excess partial entropy of Rh can be deduced from the emf,

$$\Delta S^E_{Rh} = 3F(dE/dT)_{X_{Rh}} + R \ln X_{Rh} \quad [9]$$

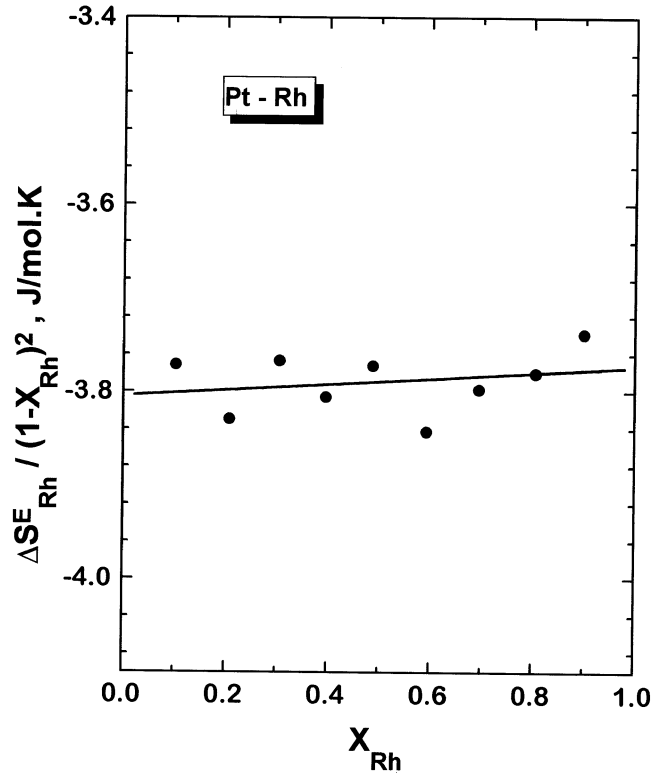

Fig. 5—Composition dependence of the function $\Delta S^E_{Rh}/(1 - X_{Rh})^2$ at a mean temperature of 1100 K.

The composition dependence of the excess partial entropy, displayed in Figure 5, can be represented by the relation

$$\Delta S^E_{Rh} = (1 - X_{Rh})^2[-3.80 + 0.031X_{Rh}] \text{ J/mol·K} \quad [10]$$

By combining the partial excess free energy at 1273 K with partial excess entropy, the partial enthalpy of Rh is obtained,

$$\Delta H_{Rh} = \Delta G^E_{Rh} + 1273 \times \Delta S^E_{Rh} = (1 - X_{Rh})^2[-10{,}970 + 90X_{Rh}] \text{ J/mol} \quad [11]$$

From the Gibbs–Duhem equation, partial excess properties of Pt and integral excess mixing properties are derived,

$$\Delta S^E_{Pt} = X^2_{Rh}\,[-3.8155 + 0.031X_{Rh}] \text{ J/mol·K} \quad [12]$$

$$\Delta S^E = X_{Rh}\,(1 - X_{Rh})[-3.80 + 1.55 \times 10^{-2}\, X_{Rh}] \text{ J/mol·K} \quad [13]$$

$$\Delta H_{Pt} = X^2_{Rh}[-11{,}015 + 90X_{Rh}] \text{ J/mol} \quad [14]$$

$$\Delta H = X_{Rh}\,(1 - X_{Rh})[-10{,}970 + 45X_{Rh}] \text{ J/mol} \quad [15]$$

The derived enthalpy and entropy values correspond to a mean temperature of 1100 K. It would be useful to confirm the derived enthalpy of mixing by a calorimetric technique. The integral excess properties are plotted as a function of composition in Figure 6. The sign of the excess entropy is the same as that of the enthalpy of mixing. Hence, only a fraction of the enthalpy of mixing is manifested as excess free energy at high temperatures. The negative deviation from ideality decreases with increasing temperature.

The enthalpy of mixing obtained in this study can be compared with values calculated using the semiempirical models of Miedema *et al.*[12] and Colinet *et al.*[13] According

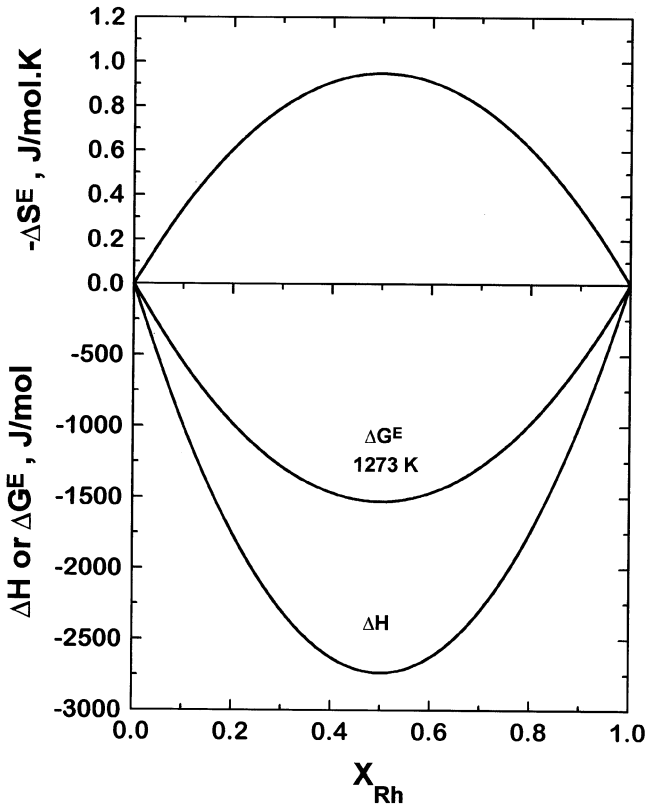

Fig. 6—Composition dependence of integral molar excess functions for solid Pt-Rh alloys.

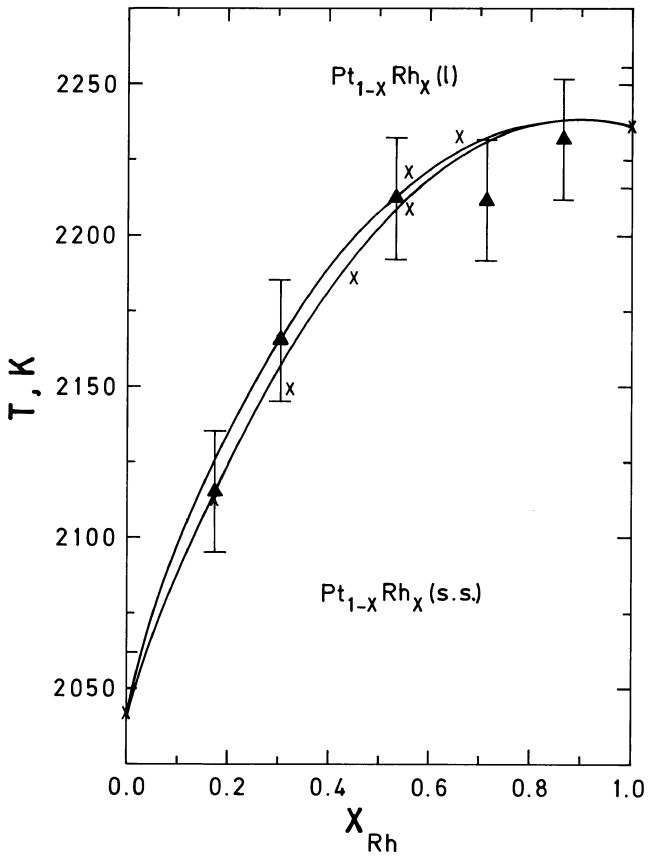

Fig. 7—Comparison of the computed liquidus and solidus for the system Pt-Rh with melting temperatures reported in the literature: x–Müller[2]; and ▲—Acken.[3]

to the model of Miedema and coworkers, the enthalpy of mixing of binary alloys of transition metals is given by

$$\Delta H = [-Pe(\Delta\phi)^2 + Q(\Delta n_{WS}^{1/3})^2]\, f(c) \qquad [16]$$

where P and Q are constants. The value of P depends on the type of metals (transition or nontransition) forming the alloy. For alloys of transition metals, $P = 14.1$. The value of $Q/P = 9.4$ is the same for all alloys. The concentration dependence of ΔH is given by $f(c)$. For ordered compounds at an equiatomic composition, its value is 0.375.[12] The value of $f(c)$ is 0.25 for a disordered alloy of the same composition. The first term in Eq. [16] gives a negative contribution arising from the requirement of equality for the chemical potential for electrons in different Wigner–Seitz (WS) cells of the alloy, similar to the electronegativity factor given by Pauling.[14] The second term gives a positive contribution, related to the difference in density of electrons at the boundary of the WS cells. The values[12] for the electronegativity parameter ϕ (in volts) and the density parameter n_{ws} (in density units) are

Element	ϕ	$n_{ws}^{1/3}$
Pt	5.65	1.78
Rh	5.40	1.76

The calculated value of heat of formation for an ordered phase of equiatomic composition is −1.7 kJ/g-at. For a disordered alloy, the corresponding value is −1.1 kJ/g-at. Colinet *et al.*[13] used a tight binding scheme for the *d*-band to evaluate the enthalpies of formation for transition metal alloys. Input parameters of the model are the atomic energy levels and bandwidths. Optimum values for the parameters were obtained by fitting known values for enthalpies of formation of transition metal alloys.[13] For an ordered Pt-Rh alloy of equiatomic composition, the model predicts an enthalpy of formation of −4 kJ/mol.[13] Thus, the negative heat of formation obtained in this study is consistent with the predictions of semiempirical models of alloy formation.

B. *Phase Diagram for the Pt-Rh System*

Since the enthalpy of mixing has a relatively large negative value and the excess entropy is negative, the system does not exhibit solid-state immiscibility. Raub[6] has estimated the critical temperature for solid-state immiscibility using a nonlinear correlation between the critical temperature and the difference in melting points of the pure elements forming the alloy. The correlation was established using experimental information on three systems: Pt-Ir, Pd-Ir, and Pd-Rh. There is no theoretical justification for this correlation.

Assuming the liquid solution to be ideal, the solidus and liquidus temperatures can be calculated from the thermodynamic data for solid alloys obtained in this study. For solid-liquid equilibria, the chemical potential of each component at the solidus composition is equal to the chemical potential at the liquidus at constant temperature; $\mu_{Pt}^{s} = \mu_{Pt}^{l}$ and $\mu_{Rh}^{s} = \mu_{Rh}^{l}$. Expressing the chemical potential in the solid phase as a sum of ideal and excess components, one obtains the following equations containing two unknown compositions:

$$\ln (X^l_{Rh}/X^s_{Rh}) = ((\mu^o_{Rh(s)} - \mu^o_{Rh(l)})/RT) + (\Delta G^E_{Rh(s)}/RT) \quad [17]$$

$$\ln \{(1 - X^l_{Rh})/(1 - X^s_{Rh})\} = ((\mu^o_{Pt(s)} - \mu^o_{Pt(l)})/RT) + (\Delta G^E_{Pt(s)}/RT) \quad [18]$$

where X^s_{Rh} and X^l_{Rh} are the mole fractions of Rh at the solidus and liquidus compositions, respectively, at temperature T. Values for the difference in chemical potential of the pure metal i (μ^o_i) in the solid and liquid states are computed using data from Knacke *et al.*[15] The constant value given for the heat capacity of the liquid above the melting point is also used for the supercooled state. The solidus and liquidus compositions at selected temperatures are obtained by solving the equations using an iterative procedure. The computed curves are compared in Figure 7 with melting temperatures reported in the early literature.[2,3] The computed phase boundary curves are compatible with experimental data obtained using optical pyrometry, especially in view of the large uncertainty (± 20 K) in temperature measurement. The temperature difference between the computed solidus and liquidus becomes insignificant for Rh-rich alloys. If the phase boundaries can be determined accurately, it will be possible to check the assumption of ideal behavior for liquid alloys. Conversely, if the thermodynamic properties of liquid alloys become available, the phase boundary curves can be computed with greater accuracy.

Pt-Rh alloys are used as heating elements for furnaces that operate at temperatures higher than can be reached with pure Pt. An alloy containing 80 at. pct Rh is the most suitable from the point of view of melting temperature. However, this composition is relatively more expensive and difficult to work. Significant improvements in melting temperature can be achieved by alloying up to 40 at. pct Rh. Wires of Pt-Rh alloys with 40 at. pct Rh are more easy to fabricate. This composition is also characterized by a high value for electrical resistivity and a relatively low value for the temperature coefficient of resistance.

IV. CONCLUSIONS

The thermodynamic mixing properties for the Pt-Rh system, determined by emf measurements on solid galvanic cells, clearly establish the absence of any solid-state miscibility gap. Activities exhibit negative deviation from Raoult's law; the extent of deviation decreases with increasing temperature. The relative excess partial molar Gibbs energies (ΔG^E_i) or chemical potentials ($\Delta \mu^E_i$) derived from emf measurements can be represented by the following equations as a function of temperature and composition:

$$\Delta \mu^E_{Rh} = \Delta G^E_{Rh} = (1 - X_{Rh})^2 [(-10{,}970 + 3.80\ T) + (90 - 0.031\ T)\ X_{Rh}] \quad \text{J/mol}$$

$$\Delta \mu^E_{Pt} = \Delta G^E_{Pt} = X^2_{Rh} [(-11{,}015 + 3.8155\ T) + (90 - 0.031\ T)\ X_{Rh}] \quad \text{J/mol}$$

REFERENCES

1. *Binary Alloy Phase Diagrams*, T.B. Massalski, P.R. Subramanian, H. Okamoto, and L. Kaeprzak, eds., ASM INTERNATIONAL, Materials Park, OH, 1990, vol. 3.
2. L. Müller: *Ann. Phys.*, 1930, vol. 7, pp. 9-47.
3. J.S. Acken: *J. Res. Bur. Standards*, 1934, vol. 12, pp. 249-58.
4. P.M. Hansen: *Constitution of Binary Alloys*, 2nd ed., McGraw-Hill Book Co. Inc., New York, NY, 1958.
5. W.G. Moffatt: *Handbook of Binary Phase Diagrams*, Business Growth Services, General Electric Co., Schenectady, NY, 1976 and updates.
6. E. Raub: *J. Less-Common Met.*, 1959, vol. 1, pp. 3-18.
7. A.S. Darling: *Platinum Met. Rev.*, 1961, vol. 5, pp. 58-65.
8. R.P. Elliott: *Constitution of Binary Alloys*, 1st suppl., McGraw-Hill Book Co., New York, NY, 1965, p. 748.
9. E. Raub and G. Falkenburg: *Z. Metallkd.*, 1964, vol. 55, pp. 392-97.
10. K.T. Jacob and M.V. Sriram: *Metall. Mater. Trans. A*, 1994, vol. 25A, pp. 1347-57.
11. R.A. Rapp and F. Maak: *Acta Metall.*, 1962, vol. 10, pp. 63-69.
12. A.R. Miedema, P.F. de Chatel, and F.R. de Boer; *Phys. B*, 1980, vol. 100, pp. 1-28.
13. C. Colinet, A. Pasturel, and P. Hicter: *CALPHAD*, 1985, vol. 9, pp. 71-99.
14. L. Pauling: *The Nature of the Chemical Bond*, 3rd ed., Cornell University Press, New York, NY, 1960, pp. 76-228.
15. O. Knacke, O. Kubaschewski, and K. Hesselmann: *Thermochemical Properties of Inorganic Substances*, 2nd ed., Springer-Verlag, Berlin, 1991, vols. I–II, pp. 1616-88.